# REPORT DOCUMENTATION PAGE

*Form Approved*
*OMB No. 0704-0188*



1. AGENCY USE ONLY *(Leave blank)*

2. REPORT DATE
07/00/79

3. REPORT TYPE AND DATES COVERED

4. TITLE AND SUBTITLE
TEST ON SELECTED ALUMINAS TO DETERMINE PSEUDO KINETIC RATE CONSTANTS AND CHARACTERIZE ADSORPTION CURVES IN SUPPORT OF ITARMS, TASK NO. 1.05.15

5. FUNDING NUMBERS

6. AUTHOR(S)
PRUSINSKI, D.

7. PERFORMING ORGANIZATION NAME(S) AND ADDRESS(ES)
ROCKY MOUNTAIN ARSENAL (CO.)
COMMERCE CITY, CO

8. PERFORMING ORGANIZATION REPORT NUMBER
81325R20



9. SPONSORING/MONITORING AGENCY NAME(S) AND ADDRESS(ES)

10. SPONSORING/MONITORING AGENCY REPORT NUMBER

11. SUPPLEMENTARY NOTES

12a. DISTRIBUTION/AVAILABILITY STATEMENT

APPROVED FOR PUBLIC RELEASE; DISTRIBUTION IS UNLIMITED

12b. DISTRIBUTION CODE

13. ABSTRACT *(Maximum 200 words)*

THE NEED TO FIND KINETIC RATE CONSTANTS FOR SELECTED ALUMINAS WAS GENERATED FROM PREVIOUS ALUMINA COLUMN STUDIES PERFORMED AT ROCKY MOUNTAIN ARSENAL. THE PROBLEM THAT HAD NOT BEEN ADDRESSED WAS FINDING A MEANS OF CALCULATING THE INITIAL FLUORIDE REMOVAL BY ALUMINAS BEFORE THE LINEAR PORTION OF THE FLUORIDE BREAK-THROUGH CURVE HAD BEEN REACHED SIX ALUMINAS WERE CHOSEN FOR PSEUDO-KINETIC RATE CONSTANT TEST RUNS. EXPERIMENTAL AND MATHEMATICAL METHODOLOGY ARE GIVEN IN THE PROCEDURE SECTION.



14. SUBJECT TERMS
MATHEMATICAL PROCEDURES

15. NUMBER OF PAGES

16. PRICE CODE

17. SECURITY CLASSIFICATION OF REPORT
UNCLASSIFIED

18. SECURITY CLASSIFICATION OF THIS PAGE

19. SECURITY CLASSIFICATION OF ABSTRACT

20. LIMITATION OF ABSTRACT

19951218 067

PER QUINTON DURST (303 289-0471) AT THE

DEPT OF ARMY, ROCKY MOUNTAIN ARSENAL

COMMERCE CITY, CO. , HIS COPY IS THE SAME

FIGURE 17 IS CUT OFF AND FIGURES 22 AND 23

ARE MISSING.

JANUARY 31, 1996

DRAFT

Don Campbell

original 81325R20

# TEST ON SELECTED ALUMINAS TO DETERMINE PSUEDO-KINETIC RATE CONSTANTS AND CHARACTERIZE ADSORPTION CURVES



IN SUPPORT OF ITARMS TASK NO. 1.05.15

BY

DENNIS M. PRUSINSKI, Ch. E., P, D & E, C.M., RMA

ROCKY MOUNTAIN ARSENAL

COMMERCE CITY, CO 80022



JULY 1979

APPROVAL:

CARL G. LOVEN
Chemical Engineer
Process Development and Engineering Branch
Industrial Division

File

File

[redacted]

## PURPOSE

The tests performed prior to this test run established the technical and economic feasibility of efficient fluoride removal via alumina column adsorption. This followed with second generation research effort that has or is being completed on aluminas column adsorption modes, but the derivation of a predictive mathematical model for alumina columns had not been made. These tests were made to find a predictive mathematical model for alumina columns. This predictive model uses a psuedo-kinetic rates constant, rate expression which enables alumina column behavior to be predicted for selected aluminas. The predicted behavior (theoretical) can then be compared to the actual behavior to determine if the actual behavior follows the predictive behavior. Significant deviations would indicate either an alumina column plant malfunction and/or misadjusted; thus an early diagnosis (warning) could be made of plant failure and subsequent fix would greatly shorten downtime and improve the overall plant efficiency.

## DETERMINATION OF KINETIC RATE CONSTANTS IN ALUMINA ADSORPTION FOR SELECTED ALUMINAS

### INTRODUCTION

The need to find kinetic rate constants for selected aluminas was generated from the alumina column test results at Rocky Mountain Arsenal. The problem that had not been addressed was finding a means of calculating the initial fluoride removal by aluminas before the linear portion of the fluoride removal versus gallonage curve had been reached. It is important especially with alumina adsorption columns to define the above mentioned region. The reason is improper switching of alumina adsorption columns* could result in a loss in efficiency. Information about the region before linear fluoride removal was reached would reduce the loss inefficiency, accordingly, test runs were scheduled. Since it was not known which of the available aluminas would be used in the final design configuration, six aluminas were chosen for a pseudo-kinetic** rate constant test runs. The rate adsorption constants and rate expressions derived would allow the prelinear region to be approximated closely. The proper switching of alumina columns could then be made based on the values for the items above. The experimental and mathematical methodology are given in the procedure section.

* It is anticipated two or mole alumina columns will be needed to allow a regeneration cycle to be performed, especially if pH adjustment used.

** pseudo-kinetic or apparent rate; the rate of adsorption is actually much faster.

EXPERIMENTAL PROCEDURE

The items needed to determine a kinetic rate adsorption constant and a rate expression are the initial concentration ($C'_{ao}$) and the concentrations ($C'_a$) at set elapsed times (t). The generalized rate expression is $+rA = \frac{-dC'_a}{dt}$, that is $+rf = \frac{-dC'_a}{dt} = kf\,(C'_a)$ with rf the pseudo-kinetic rate of adsorption; $C'_a$ the concentration at time t. The intergrated rate expression is then $\int dC'_a/f(C'_a) = -k\int dt$ with k the kinetic rate constant and t the elapsed time. Temperaure, pressure and alumina dosage were maintained constant with time of contact being varied. The alumina dosage was selected so that inter-ionic competition would be minimized between fluoride ions.

To find $C'_{ao}$ and $C'_a$ at t each rate test was done in the following manner:

(1) Eight jars received 5 grams of the alumina being tested with a ninth jar set aside for a control;

(2) The nine jars were filled with 800 ml of Calgon plant effluent water, placed in a constant temperature bath with agitators started;

(3) Each hour a jar was removed and immediately filtered to 'stop' the adsorption action of the alumina, the control (blank) was filtered with the eight hour elapsed time sample;

(4) Fluoride concentration and pH measurements were found on the samples and recorded along with elapsed time for the sample.

## MATHEMATICAL PROCEDURE

Defining $r_F$ as the apparent rate of disappearance of fluoride ion, $C_F$ as the concentration of fluoride ion in solution and t as the time, the apparent kinetic rate is given by $\frac{-dC_F}{dt} = +r_F$ for the reduction of fluoride ion; this can also be written $\frac{-dC_F}{dt} = kf.(C_F)$. The equations given above are the generalized rate expressions, however, in order to obtain the integrated rate expression for predicting the adsorption of fluoride ions from solution, $f(C_F)$ must be found. Rearranging the pseudo-kinetic rate expression gives $\frac{-dC_F}{f(C_F)} = kdt$ so that the integrated rate expression can be found, when f $(C_F)$ known, by integration. One method is to assume $f(C_F)$ has the form $C_F^N$ where N = 0, 1/G, 1, G (G = real number) which limits the form of the integrated pseudo-kinetic rate expression to four forms. The four integrated pseudo-kinetic rate expressions are then:

(1) $C_{ao}$ = initial concentration and $C_a$ = concentration at time t.
$(C_a - C_{ao}) = -kt + I_c$ ($I_c$ - constant of integration),

(2) $G\,(C_a^{1/G} - C_{ao}^{1/G}) = -kt + I_c$ ,

(3) $\ln (C_a/C_{ao}) = -kt + I_c$ and

(4) $1/G\,(C_a^{-G+1} - C_{ao}^{-G+1}) = -kt + I_c$

Now $C_{ao}$ (the initial concentration) is a constant and the $C_{ao}$ terms $(e - C_{ao}^{1/n})$ are therefore constant and can be represented by $K_c$ (a constant term).

The four pseudo-kinetic rate expressions then become (after substitution and rearrangement):

(1) $C_a = K_c + I_c - kt$,

(2) $G\,C_a^{1/G} = K_c + I_c - kt$,

(3) $\ln C_a = K_c + I_c - kt$, and

(4) $\frac{1}{G} C_a^{-G+1} = K_c + I_c - kt$.

Further combining the constants $K_c$ and $I_c$ to give a new constant $J_c = K_c + I_c$ renders the four pseudo-kinetic rate expressions in the final forms:

(1) $C_a + J_c - kt$,

(2) $G\,C_a^{1/G} = K_c - kt$,

(3) $\ln C_a = J_c - kt$, and

(4) $\frac{1}{G} C_a^{-G+1} = J_c - kt$.

The problem now becomes one of selecting one of the above equations which represents the best fit to the $C_a$ versus t plot. To select the best fit, the tabulized data was taken to MISO and analyzed via a modified simple regression program. This modified simple regression program calculated the correlation coeffficient*, residuals, plotted the equation selected from the regression analysis, gave the 95% confidence bands for the linear case, and gave the k G and $I_c$ values. Since the aluminas are constrained to follow the same rate mechanism (by physical chemistry laws), it was expected one f ($C_a$) would be found which would yield a high correlation coefficient for all the aluminas.

* Correlation coefficient ($R^2$) = 1.00 - direct correlation (X = y), excellent fit; $R^2$ = -1.00 - inverse correlation (1/x = y), excellent equation fit; $R^2$ = 0.0 - no correlation, $R^2$ between 0.0 and $\pm$ 1.00 - partial correlation with stronger correlation as $R^2 \longrightarrow \pm 1.00$.

## DATA AND RESULTS OF REGRESSION ANALYSIS

The concentrations of fluoride ion found for each elapsed time for the six aluminas tested are given in Table I below:

TABLE I: CONCENTRATION OF FLUORIDE ION VERSUS ELAPSED TIME FOR SIX SELECTED ALUMINAS

| ALUMINA Elapsed Time Hours | MCB (Crushed) (Spheres) | Alcoa F-1 (Regenerated) | Alcoa F-1 (Virgin) | Kaiser A-300 (Ungraded) | Kaiser A-201 (Spheres) | Kaiser 8 Mesh (Spheres) |
|---|---|---|---|---|---|---|
| | CONCENTRATION OF FLUORIDE ION (PPM) | | | | | |
| 1 | 2.69 | 3.08 | 2.52 | 1.48 | 3.35 | 3.12 |
| 2 | 2.40 | 2.92 | 1.97 | 0.978 | 3.26 | 2.94 |
| 3 | 2.00 | 2.83 | 1.84 | 0.780 | 3.18 | 2.86 |
| 4 | 1.68 | 2.75 | 1.49 | 0.778 | 3.12 | 2.48 |
| 5 | 1.46 | 2.73 | 1.43 | 0.766 | 3.04 | 2.24 |
| 6 | 1.02 | 2.70 | 1.41 | 0.729 | 3.02 | 2.17 |
| 7 | 1.00 | 2.60 | 1.28 | 0.608 | 3.00 | 2.15 |
| 8 | 0.907 | 2.59 | 1.19 | 0.560 | 2.95 | 1.69 |
| 8 (Blank) (initial Concen) | 3.60 | 3.71 | 3.62 | 3.60 | 3.60 | 3.74 |

The regression analysis was initially performed with $C_{ao}$ (the initial concentration of fluoride ion) included. Two conclusions were drawn from an analysis of the regression calculations :

(1) overall f ($C_a$) could take any of the four forms offered previously

(2) the spheres all had $C_a = K_e \exp(-kt)$ as the 1st or 2nd best correlation.

The initial regression results with $C_{ao}$ included are given in Figures 1-6. The plots of $C_a$ vs. $K_e$ exp kt for the six aluminas given in Figures 7-12.

When it comes to adsorption, the aluminas are chemically the same but physically the aluminas are different. The aluminas fall into two physical groups, spheres and granulated powders. The great difference in immediate surface area was postulated as the primary reason the spheres followed a ln concentration (or exponential kt) form while the powders seemed to follow poorer formulations. In order to determine the behavior of the aluminas without the effect of large initially available surface area versus small initially available surface area, which occurs during the start-up of the tests, the zeroeth and first hour concentrations were deleted from the granulated powder regression analyses. Also to show that the small surface of the spheres had very little effect on the correlation coefficient, thus the fit of the equation, the zeroeth hour (initial concentration) was deleted and regressions analysis done. The plots and correlation coefficient for a minimized surface effect on the granulated powders is given in Figures 13-15 while the plots and correlation coefficients to show the miniscule surface effect on the spheres is given in Figures 16-18. As can be seen from Figures 13-15 the pseudo-kinetic rate expression takes on the form $C_a = K_e \exp(kt)$ with good correlation when the surface effect minimized. Several equations were tried in order to find the apparent kinetics for the surface area effect for the granulated powders and thus generate a predictive curve. The equation having the highest consistent correlation was $\sqrt{C_a} = K_e t^k$. The plots and correlation coefficients generated using the above equation are given in Figures 19-21. As is seen from the high correlation coefficients the above expression simulates the surface area effects quite well. By now combining the results of the previous plots, it is seen the spherical shaped aluminas fluoride removal can be simulated by $C_a = K_e \exp(kt)$ integrated rate expressions up to constant removal rate region and the granulated powder by $\sqrt{C_a} = K_e t^k$ 0-2 hours then $C_a = K_e \exp(kt)$ from 2 hours to constant removal rate region start. This is shown below in Figures 22 and 23 for spherical and granulated power aluminas, respectively.

FIGURE 22: PREDICTIVE FLUORIDE ION CONCENTRATION IN ALUMINA COLUMN VS ELAPSED TIME MODEL

FIGURE 23: PREDICTIVE FLUORIDE ION CONCENTRATION IN ALUMINA COLUMN VS ELAPSED TIME MODEL

## CONCLUSIONS

The predictive models for finding fluoride concentration during the crutial start-up (switch-over times) allow the alumina column process to be more closely monitored. Using some of the Ruebel and Hager, Inc. start-up data further verification of these predictive models was made. The plots of ln concentration vs Time and the correlation coefficients are given in Figures 24 and 25. NOTE: $\ln C_a = K_e + kt$ is equivalent to $C_a = K_e \exp(kt)$. As is seen the correlation coefficients are good considering the surface area effect was not considered in these analyses. These pseudo-kinetic rate test results are not completely conclusive without several repetitions of the tests made on the aluminas. A further pseudo-kinetic rate test coupled with column test should be made to enable fluoride removal in alumina columns to be predicted by the mathematical models found.

FIGURE 1: REGRESSION (f (CA) US kt) on ALCOA F-1 (VIRGIN)

SELECT BEST FIT

| EQUATION | A | B | RES ERROR | R-SQUARE | MAX DEVIATION |
|---|---|---|---|---|---|
| Y = A*X | 0.25505 | | 1.60905 | -6.02188 | 2.26495 |
| Y = A + B*X | 2.39714 | -0.16798 | 0.03164 | 0.86194 | 0.29083 |
| Y = A*EXP(B*X) | 2.48048 | -0.09819 | 0.02101 | 0.90832 | 0.27150 |
| Y = 1/(A + B*X) | 0.37589 | 0.05950 | 0.01312 | 0.94277 | 0.22321 |
| Y = A + B/X | 1.14479 | 1.46133 | 0.01415 | 0.93826 | 0.20810 |
| Y = A + B*LOG(X) | 2.46763 | -0.62341 | 0.00481 | 0.97900 | 0.11340 |
| Y = A*X↑B | 2.54568 | -0.35289 | 0.00389 | 0.98303 | 0.11245 |
| Y = X/(A + B*X) | -0.45532 | 0.79833 | 0.05395 | 0.76455 | 0.39533 |

EQUATION Y = A*X↑B HAS MAXIMUM R-SQUARE

EQUATION Y = A*X↑B HAS MINIMUM MAXIMUM ABSOLUTE RESIDUAL

FIGURE 2: REGRESSION (f (CA) US kt) on ALCOA F-1 (REGENERATED)

SELECT BEST FIT

| EQUATION | A | B | RES ERROR | R-SQUARE | MAX DEVIATION |
|---|---|---|---|---|---|
| Y = A*X | 0.54564 | | 2.67071 | -85.04086 | 2.53436 |
| Y = A + B*X | 3.08714 | -0.07179 | 0.00218 | 0.92970 | 0.06464 |
| Y = A*EXP(B*X) | 3.09568 | -0.02544 | 0.00195 | 0.93711 | 0.06209 |
| Y = 1/(A + B*X) | 0.32198 | 0.00904 | 0.00174 | 0.94380 | 0.05903 |
| Y = A + B/X | 2.61403 | 0.50207 | 0.00324 | 0.89556 | 0.09575 |
| Y = A + B*LOG(X) | 3.08291 | -0.23230 | 0.00067 | 0.97838 | 0.04088 |
| Y = A*X↑B | 3.08871 | -0.08172 | 0.00074 | 0.97631 | 0.04461 |
| Y = X/(A + B*X) | -0.06135 | 0.38086 | 0.00394 | 0.87316 | 0.09752 |

EQUATION Y = A + B*LOG(X) HAS MAXIMUM R-SQUARE

EQUATION Y = A + B*LOG(X) HAS MINIMUM MAXIMUM ABSOLUTE RESIDUAL

FIGURE 3: REGRESSION (f (CA) US kt) on MCB SPHERES (8 X 14)

SELECT BEST FIT

| EQUATION | A | B | RES ERROR | R-SQUARE | MAX DEVIATION |
|---|---|---|---|---|---|
| Y = A*X | 0.23474 | | 2.26210 | -3.27508 | 2.45526 |
| Y = A + B*X | 2.85754 | -0.26954 | 0.02059 | 0.96109 | 0.22032 |
| Y = A*EXP(B*X) | 3.25475 | -0.16843 | 0.00757 | 0.98570 | 0.16478 |
| Y = 1/(A + B*X) | 0.19413 | 0.11385 | 0.06425 | 0.87857 | 0.55698 |
| Y = A + B/X | 0.95566 | 2.02795 | 0.11508 | 0.78251 | 0.43036 |
| Y = A + B*LOG(X) | 2.88529 | -0.93595 | 0.02349 | 0.95560 | 0.19529 |
| Y = A*X↑B | 3.21502 | -0.56250 | 0.08371 | 0.84181 | 0.52502 |
| Y = X/(A + B*X) | -0.73398 | 0.95580 | 0.74589 | -0.40963 | 1.81831 |

EQUATION Y = A*EXP(B*X) HAS MAXIMUM R-SQUARE

EQUATION Y = A*EXP(B*X) HAS MINIMUM MAXIMUM ABSOLUTE RESIDUAL

FIGURE 4: REGRESSION (f (CA) US kt) on KAISER A-201 (SPHERES)

SELECT BEST FIT

| EQUATION | A | B | RES ERROR | R-SQUARE | MAX DEVIATION |
|---|---|---|---|---|---|
| Y = A*X | 0.53632 | | 3.13162 | -120.78396 | 2.81368 |
| Y = A + B*X | 3.37714 | -0.05964 | 0.00081 | 0.96836 | 0.04036 |
| Y = A*EXP(B*X) | 3.38473 | -0.01912 | 0.00071 | 0.97252 | 0.03930 |
| Y = 1/(A + B*X) | 0.29469 | 0.00614 | 0.00062 | 0.97606 | 0.03838 |
| Y = A + B/X | 2.95507 | 0.45237 | 0.00511 | 0.80121 | 0.11161 |
| Y = A + B*LOG(X) | 3.38305 | -0.20693 | 0.00100 | 0.96116 | 0.05276 |
| Y = A*X↑B | 3.38936 | -0.06594 | 0.00117 | 0.95445 | 0.05506 |
| Y = X/(A + B*X) | -0.04545 | 0.33775 | 0.00581 | 0.77423 | 0.11142 |

EQUATION Y = 1/(A + B*X) HAS MAXIMUM R-SQUARE

EQUATION Y = 1/(A + B*X) HAS MINIMUM MAXIMUM ABSOLUTE RESIDUAL

FIGURE 5: REGRESSION (f (CA) US kt) on KAISER 8 MESH (SPHERES)

SELECT BEST FIT

| EQUATION | A | B | RES ERROR | R-SQUARE | MAX DEVIATION |
|---|---|---|---|---|---|
| Y = A*X | 0.39358 | | 3.05211 | -10.11350 | 2.72642 |
| Y = A + B*X | 3.32786 | -0.19369 | 0.01202 | 0.95623 | 0.17798 |
| Y = A*EXP(B*X) | 3.47086 | -0.08079 | 0.01363 | 0.95035 | 0.17837 |
| Y = 1/(A + B*X) | 0.26684 | 0.03452 | 0.02133 | 0.92232 | 0.19822 |
| Y = A + B/X | 1.99753 | 1.35025 | 0.09107 | 0.66837 | 0.47631 |
| Y = A + B*LOG(X) | 3.31300 | -0.64632 | 0.03351 | 0.87800 | 0.27901 |
| Y = A*X↑B | 3.42238 | -0.26366 | 0.04899 | 0.82161 | 0.30238 |
| Y = X/(A + B*X) | -0.22025 | 0.49703 | 0.14342 | 0.47777 | 0.49934 |

EQUATION Y = A + B*X HAS MAXIMUM R-SQUARE

EQUATION Y = A + B*X HAS MINIMUM MAXIMUM ABSOLUTE RESIDUAL

FIGURE 6: REGRESSION (f (CA) US kt) on KAISER A-300 (UNGRADED)

SELECT BEST FIT

| EQUATION / A | B | RES ERROR | R-SQUARE | MAX DEVIATION |
|---|---|---|---|---|
| Y = A*X<br>0.12661 | | 0.48200 | -3.93601 | 1.35339 |
| Y = A + B*X<br>1.28782 | -0.10065 | 0.02673 | 0.72627 | 0.29283 |
| Y = A*EXP(B*X)<br>1.32280 | -0.11188 | 0.02166 | 0.77817 | 0.29722 |
| Y = 1/(A + B*X)<br>0.69823 | 0.13298 | 0.01725 | 0.82336 | 0.27694 |
| Y = A + B/X<br>0.50532 | 0.97005 | 0.00291 | 0.97019 | 0.06667 |
| Y = A + B*LOG(X)<br>1.35293 | -0.39082 | 0.00948 | 0.90287 | 0.14358 |
| Y = A*X↑B<br>1.38383 | -0.41384 | 0.00521 | 0.94667 | 0.09828 |
| Y = X/(A + B*X)<br>-1.06049 | 1.65694 | 0.01187 | 0.87843 | 0.19659 |

EQUATION Y = A + B/X HAS MAXIMUM R-SQUARE

EQUATION Y = A + B/X HAS MINIMUM MAXIMUM ABSOLUTE RESIDUAL

FIGURE 7: CA vs. KE exp (kt) - ALL POINTS INCLUDED

A =
2.86125421388

B =
-0.123387635828

R-SQUARE =
0.842140771894

RES ERROR
0.109493165176

MAX(ABS(RESIDUAL))
0.758745786118

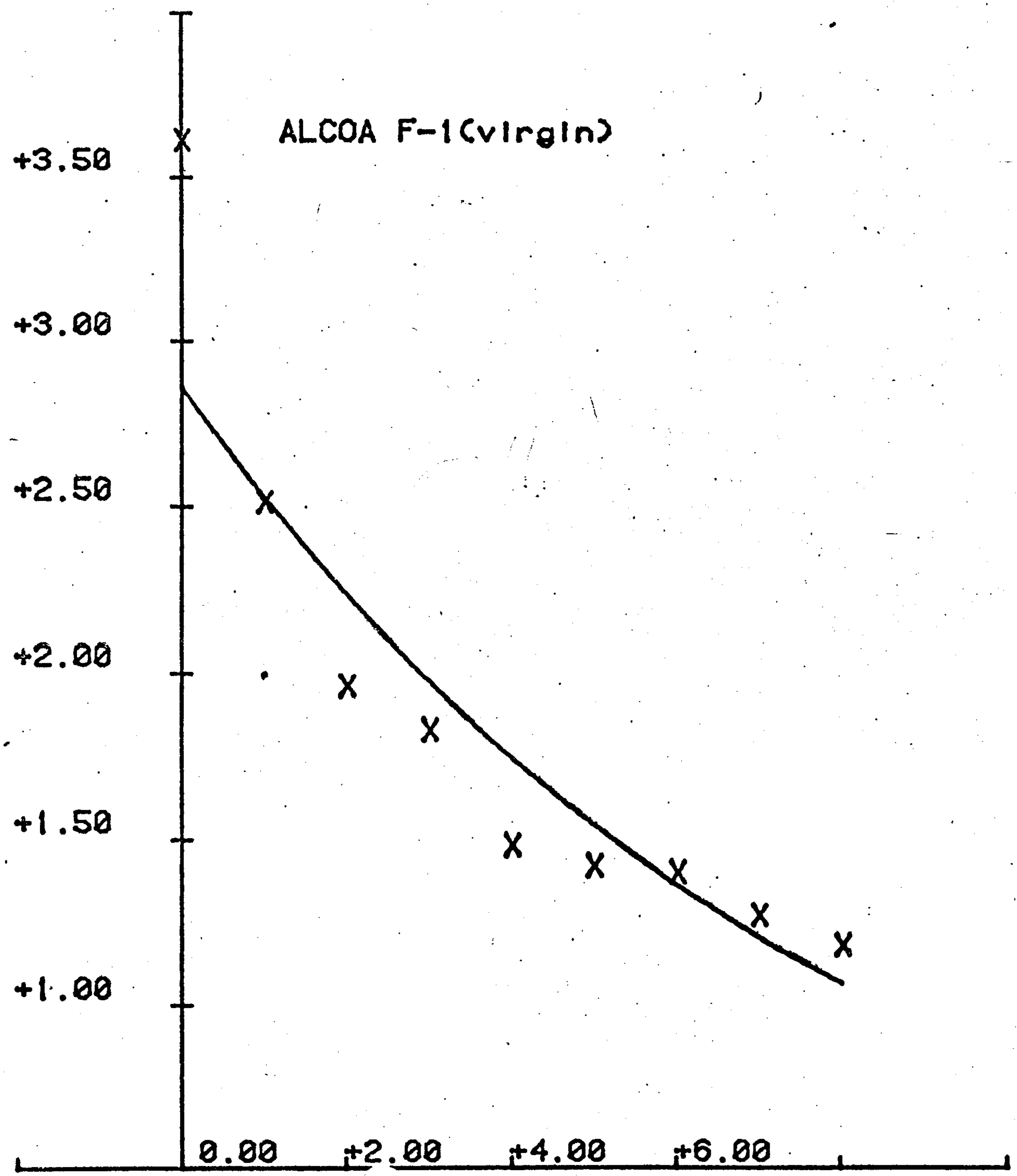

FIGURE 8: CA vs. KE exp (kt) - ALL POINTS INCLUDED.

A =
3.29984035992

B =
-0.0355755946531

R-SQUARE =
0.741570992133

RES ERROR
0.0357107868396

MAX(ABS(RESIDUAL))
0.410159640083

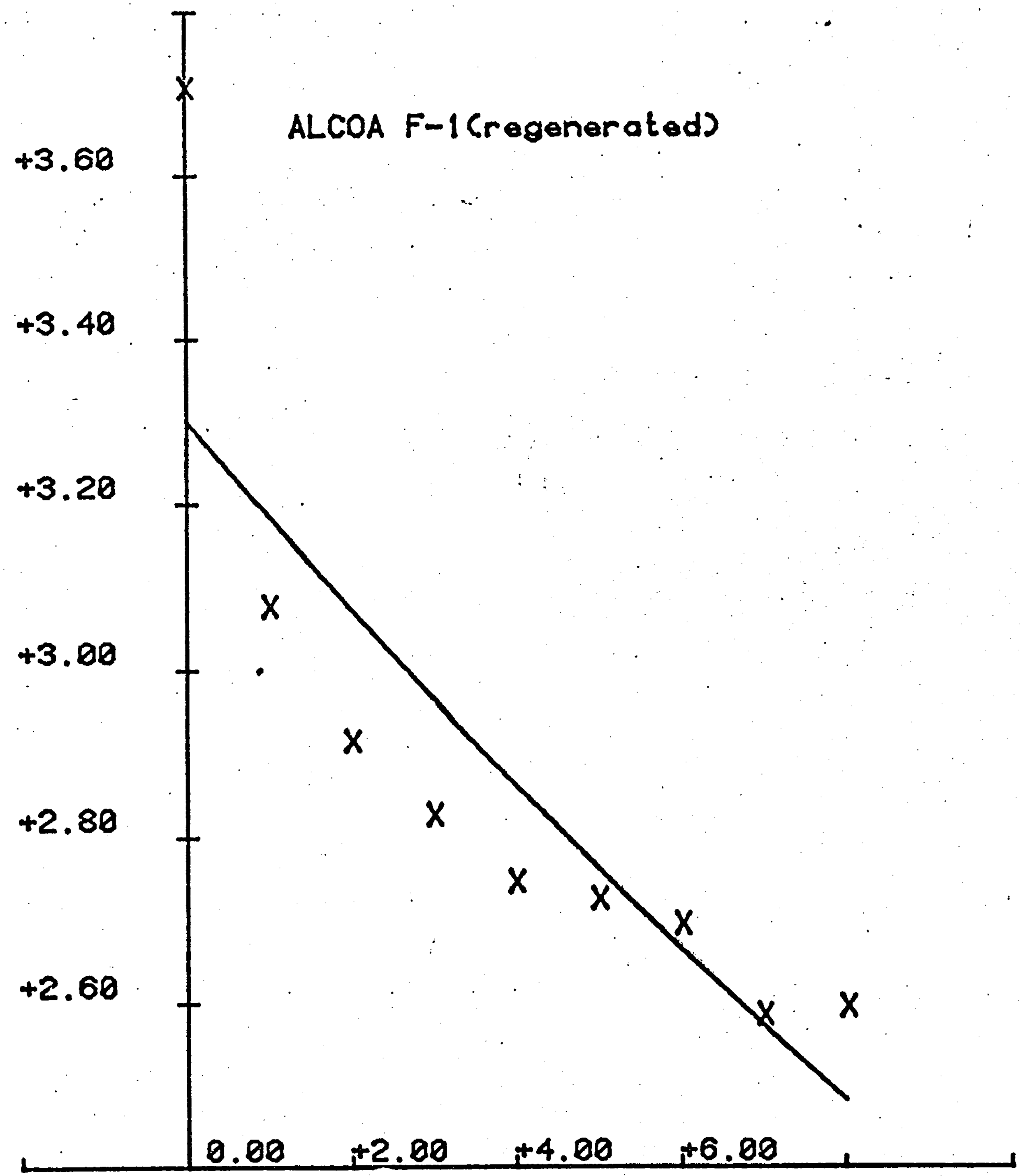

FIGURE 9; CA vs. KE exp (kt) - ALL POINTS INCLUDED

A =
3.38110489411

B =
-0.175147554052

R-SQUARE =
0.984083249635

RES ERROR
0.0149469129533

MAX(ABS(RESIDUAL))
0.218895105895

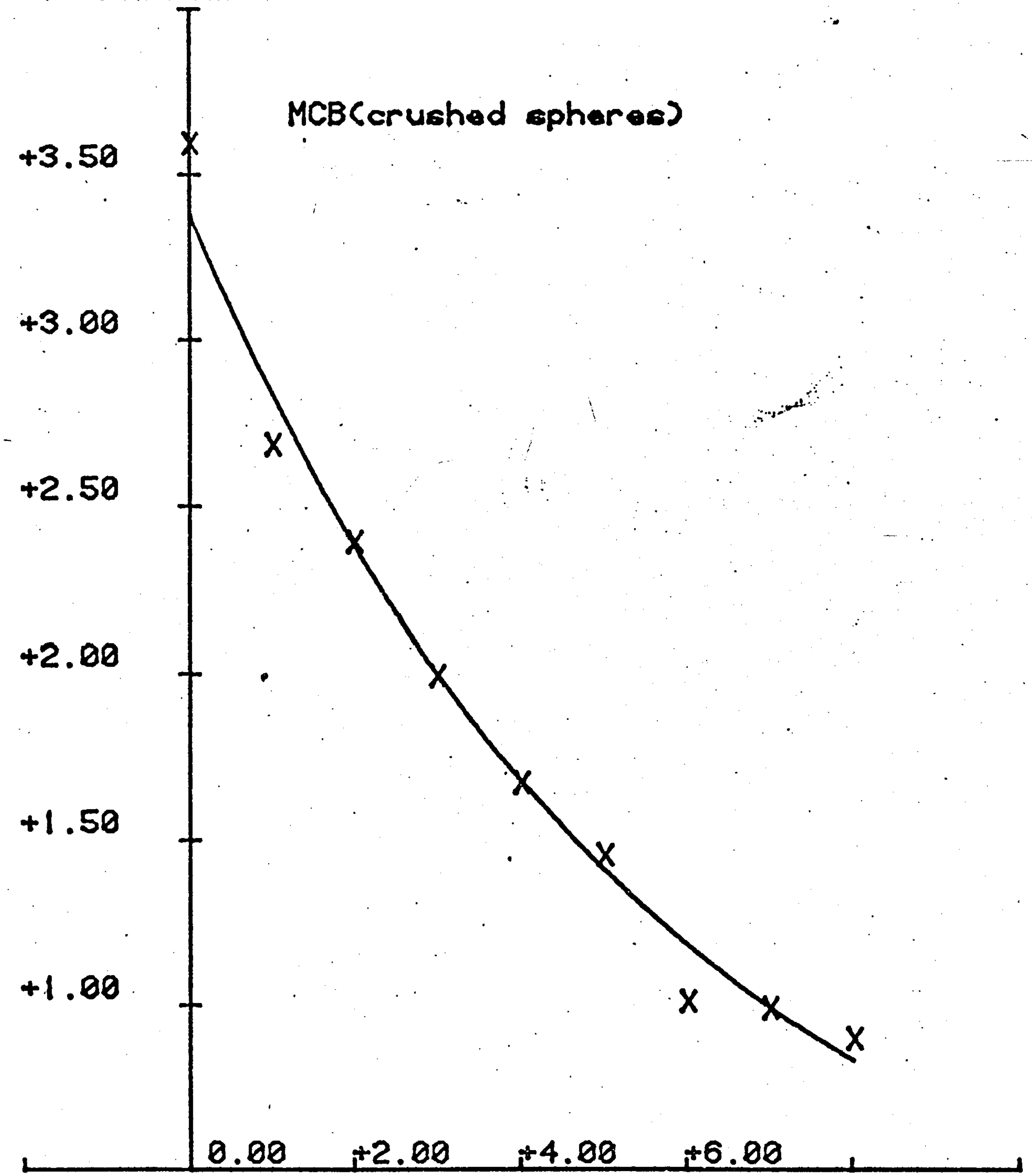

FIGURE 10: CA vs. KE exp (kt) - ALL POINTS INCLUDED.

A =
3.46449948719

B =
-0.023231683579

R-SQUARE =
0.914729365251

RES ERROR
0.00449254429933

MAX(ABS(RESIDUAL))
0.13550051281

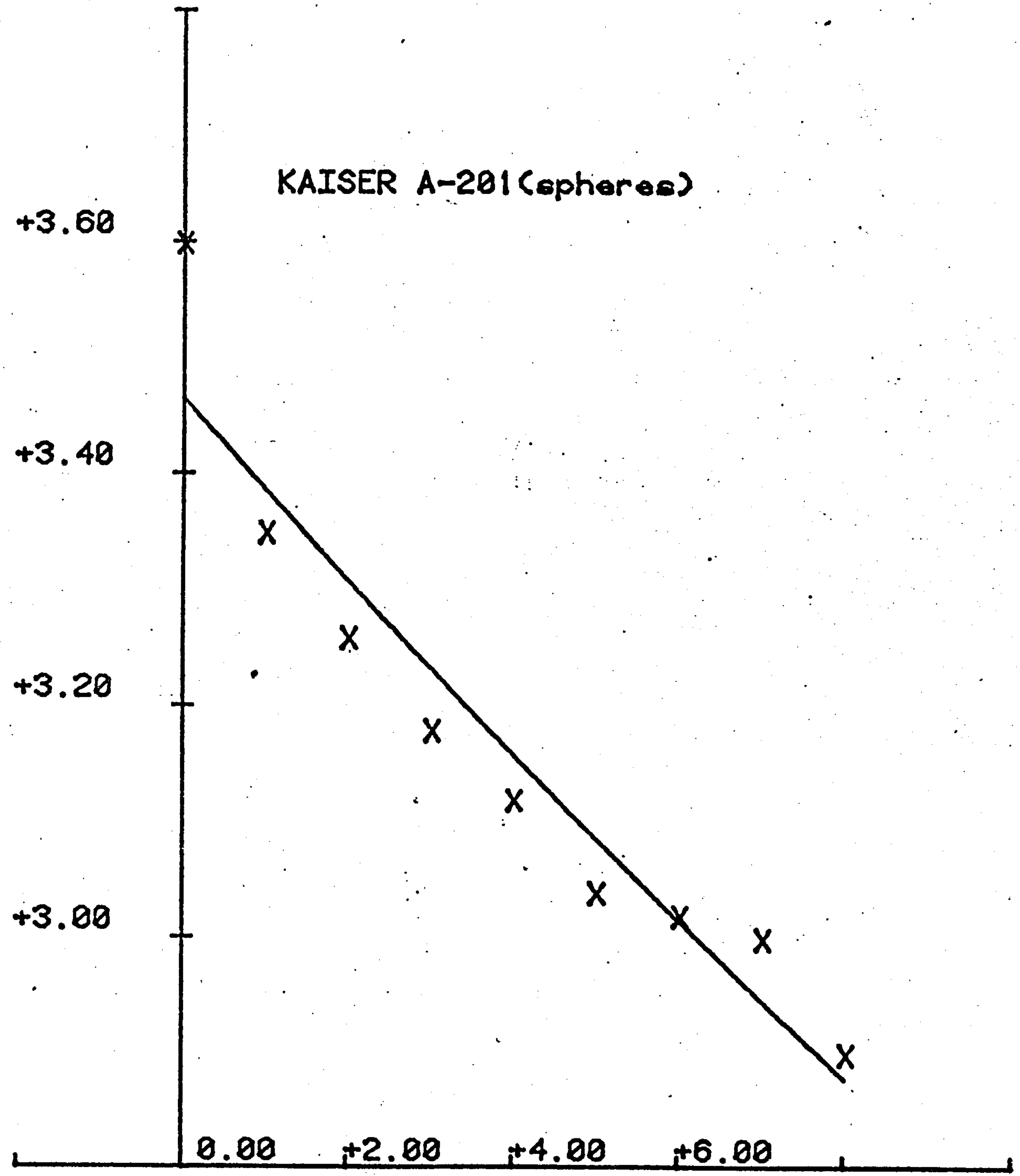

FIGURE 11; CA vs. KE exp (kt) - ALL POINTS INCLUDED.

A =
3.57018170149

B =
-0.0857705732595

R-SQUARE =
0.959037264707

RES ERROR
0.0182148930007

MAX(ABS(RESIDUAL))
0.191414599056

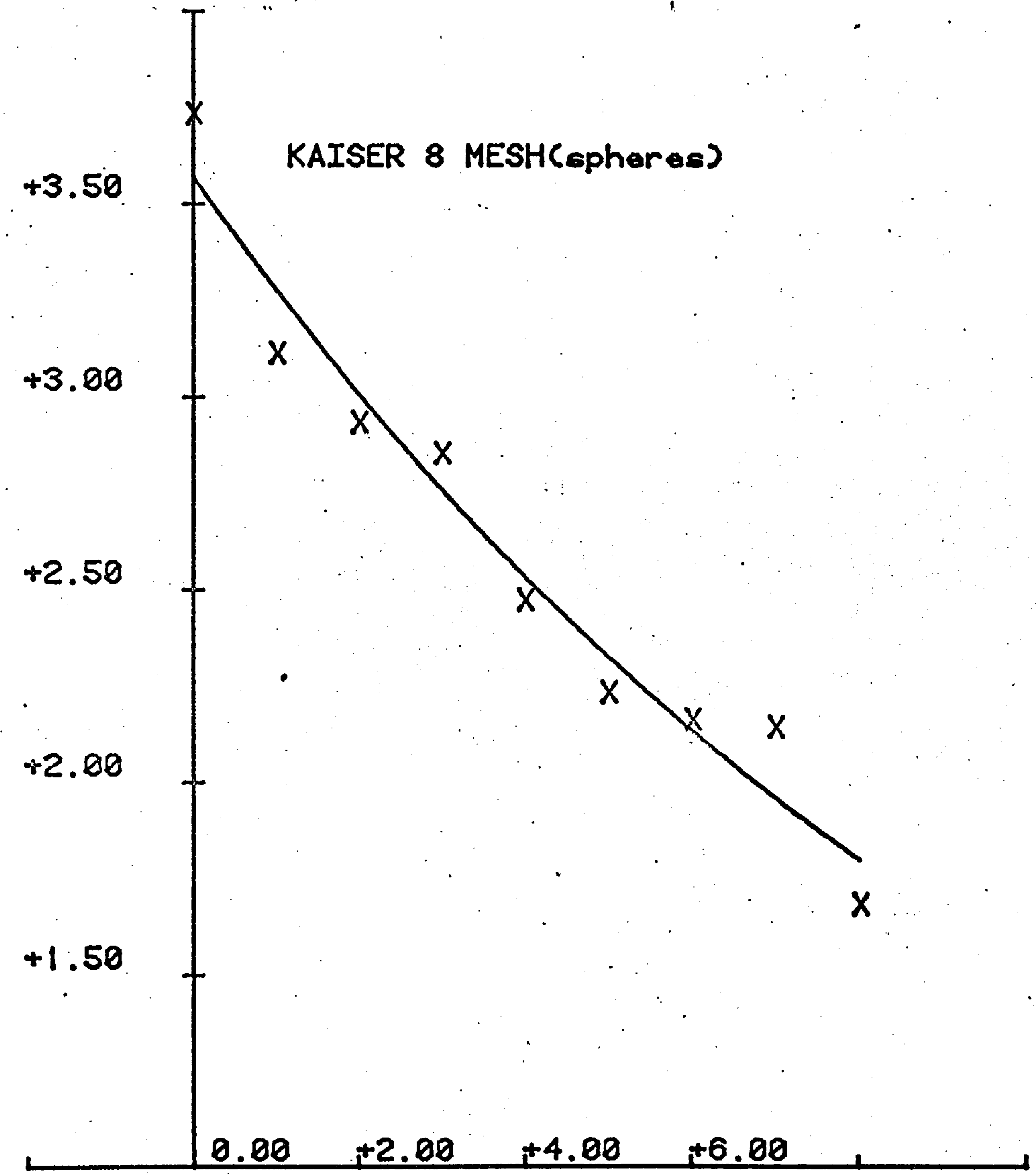

FIGURE 12: CA vs. KE exp (kt) - ALL POINTS INCLUDED.

A =
1.32280092624

B =
-0.111882177845

R-SQUARE =
0.778168813566

RES ERROR
0.0216617737619

MAX(ABS(RESIDUAL))
0.297218078377

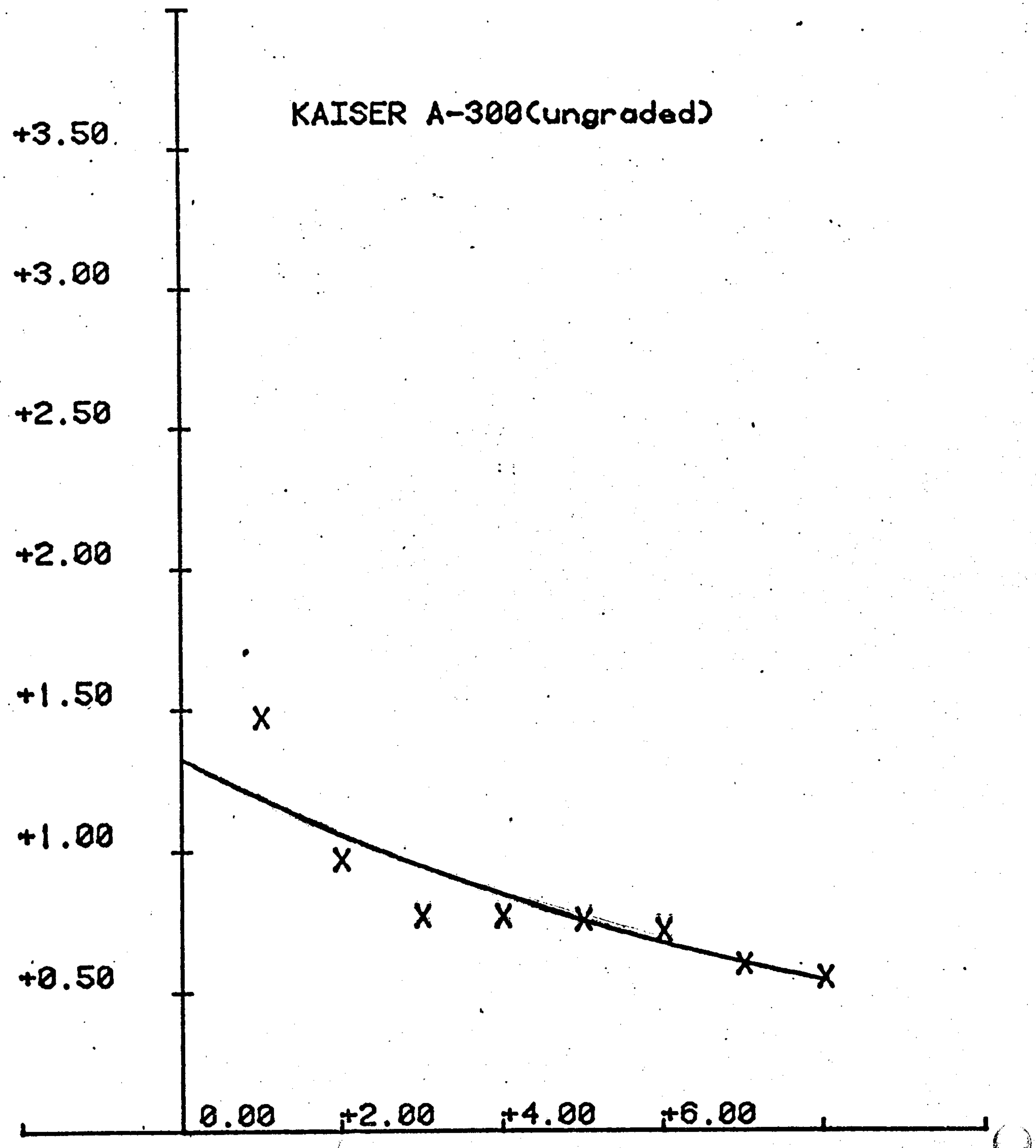

FIGURE 13:

A =
2.24957861183

B =
-0.0819013610652

R-SQUARE =
0.932718132716

RES ERROR
0.00662553382235

MAX(ABS(RESIDUAL))
0.131152750837

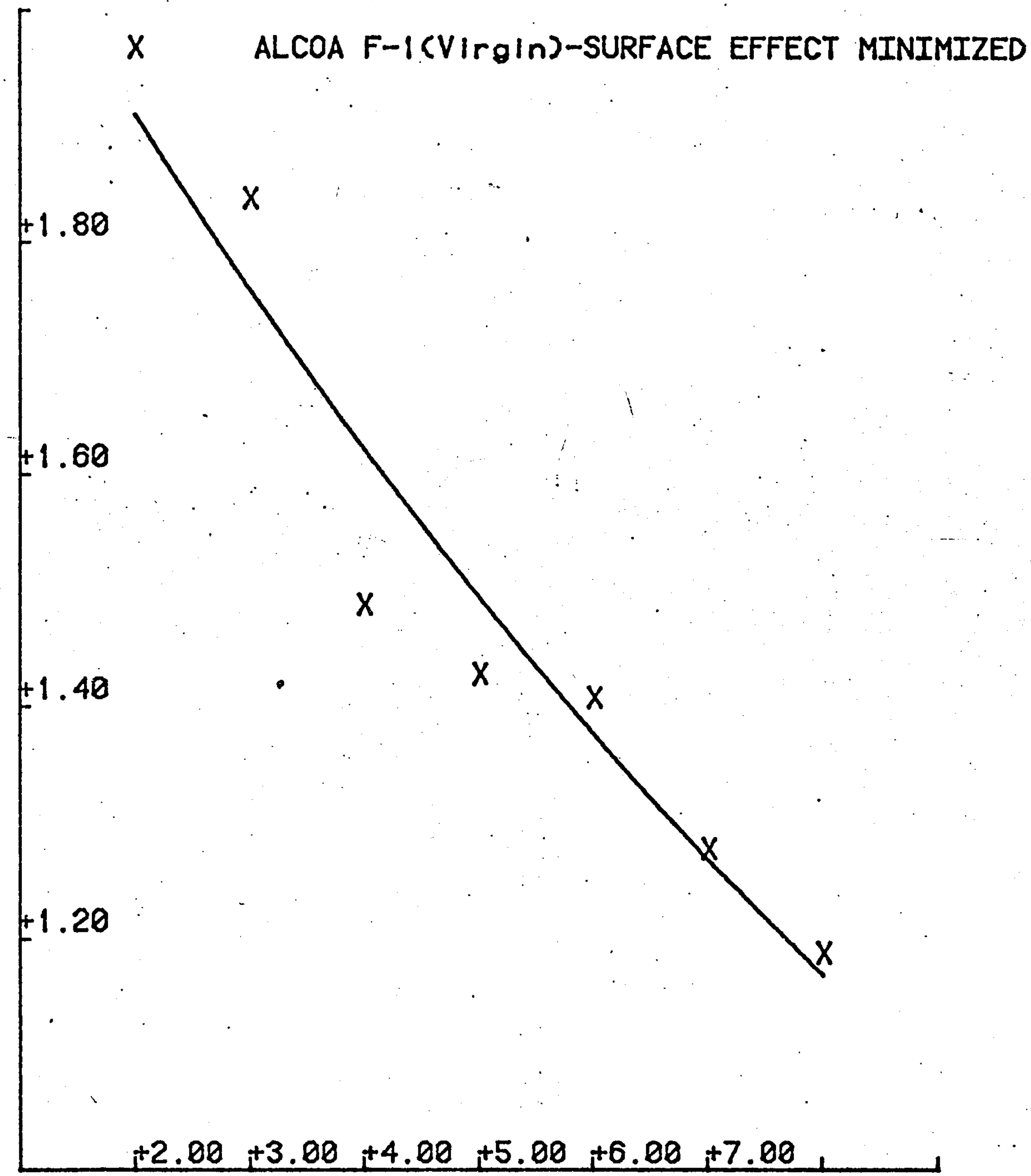

FIGURE 14:

A =
3.00964505949

B =
-0.0195591747725

R-SQUARE =
0.961163734239

RES ERROR
6.515615787E-4

MAX(ABS(RESIDUAL))
0.0331557681378

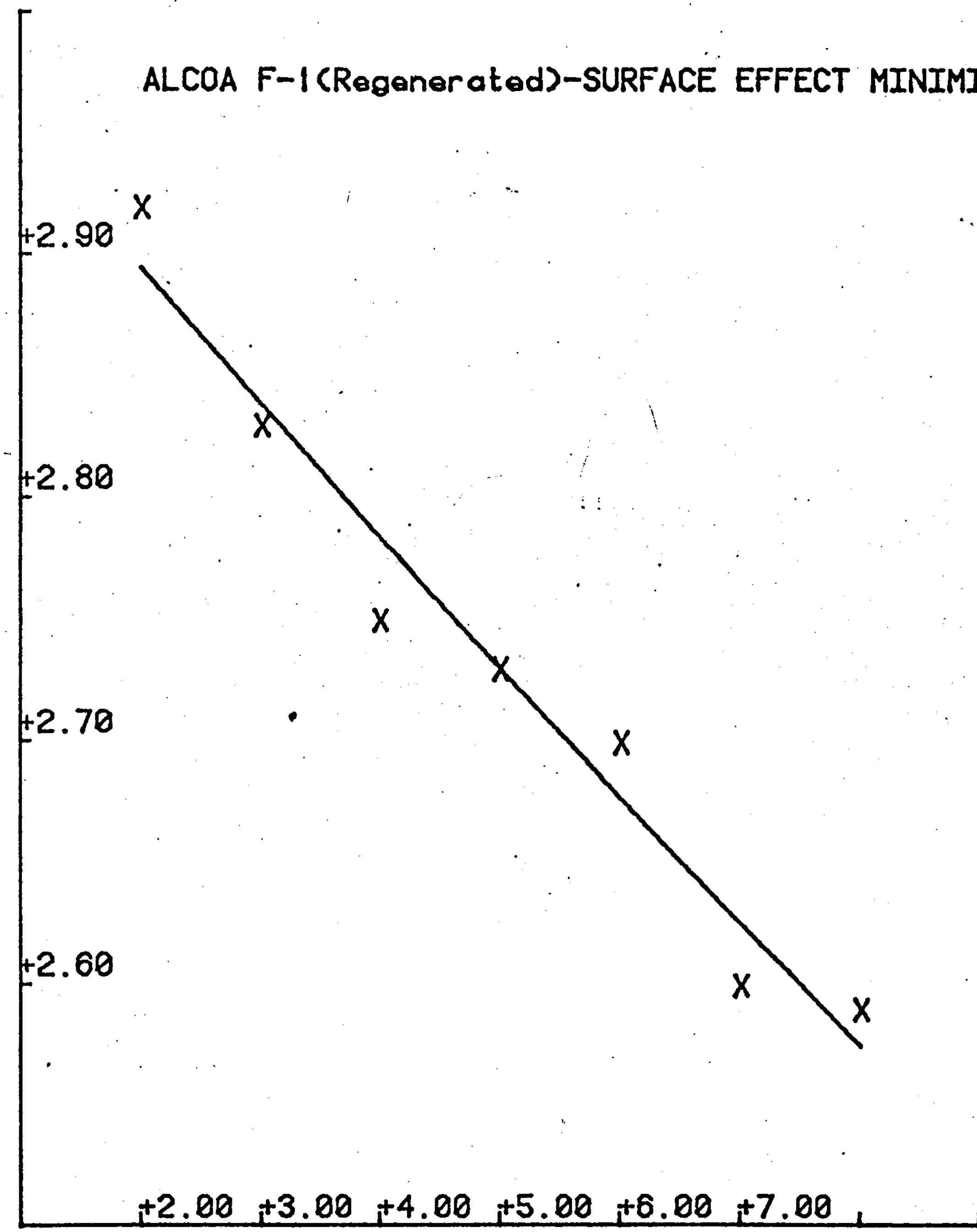

FIGURE 15:

A =
1.09155494399

B =
-0.0798574830901

R-SQUARE =
0.880220957939

RES ERROR
0.00264130583489

MAX(ABS(RESIDUAL))
0.0790147247008

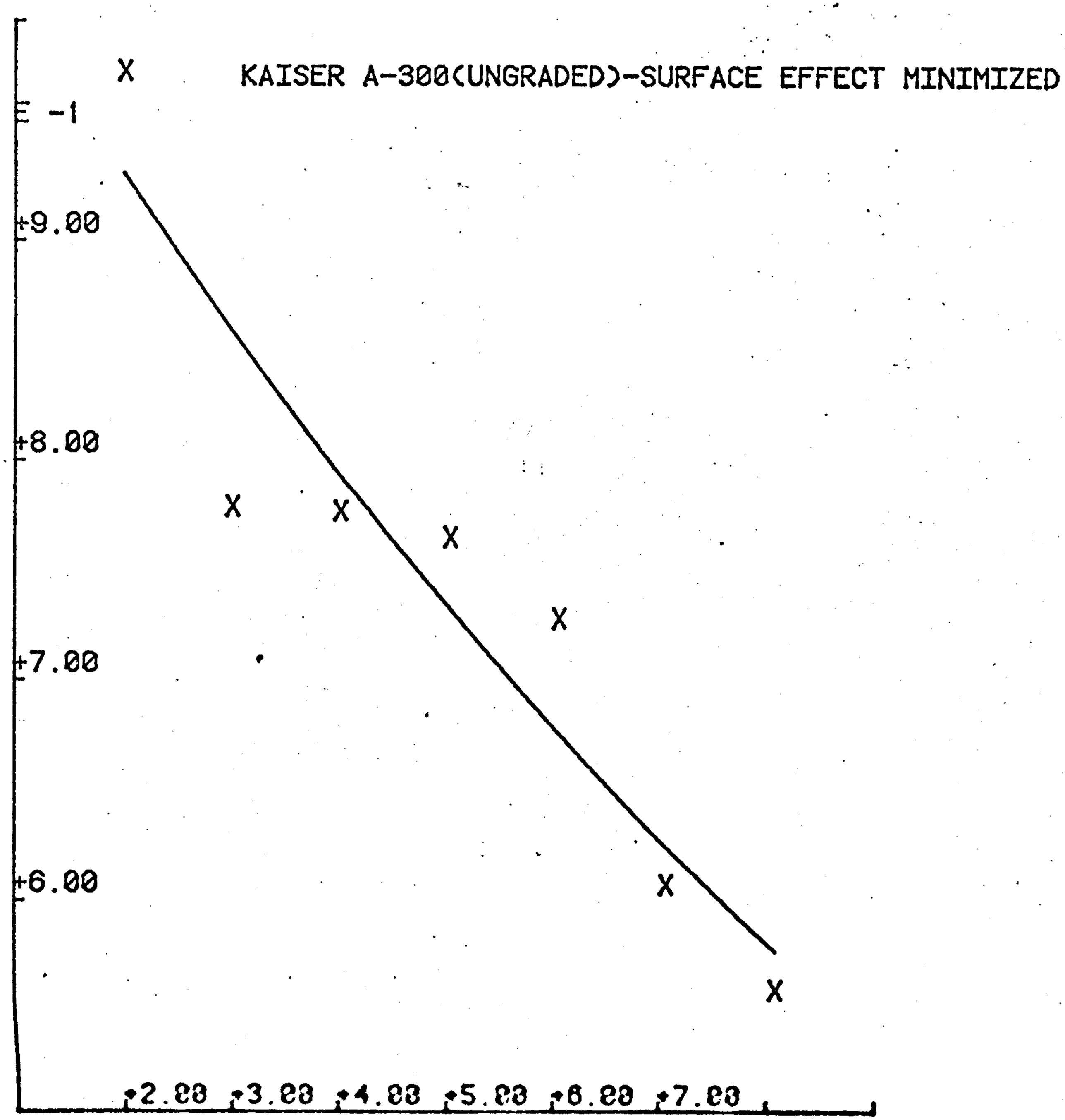

FIGURE 16: SURFACE AREA EFFECT ON KINETIC RATE EXPRESSION CORRELATION COEFFICIENT

Y = A*EXP(B*X)

A =
3.38473200105

B =
-0.0191210759296

R-SQUARE =
0.972516441289

RES ERROR
7.067282608E-4

MAX(ABS(RESIDUAL))
0.0392956408133

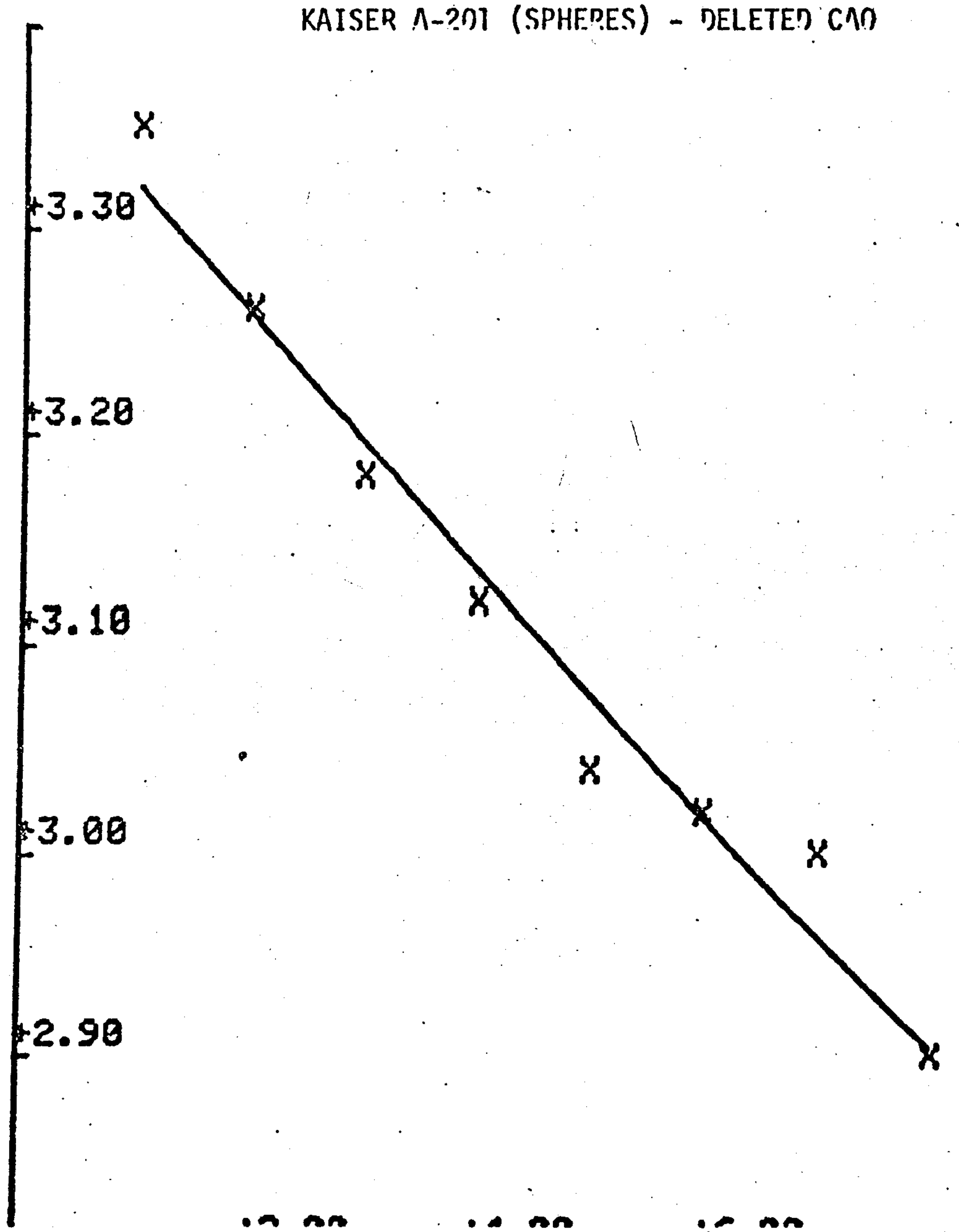

FIGURE 17: SURFACE AREA EFFECT ON KINETIC RATE EXPRESSION CORRELATION COEFFICIENT

=
3.53269923114

=
-0.0881497125267

-SQUARE =
0.974353713247

ES ERROR
0.00793154161634

AX(ABS(RESIDUAL))
0.148198712349

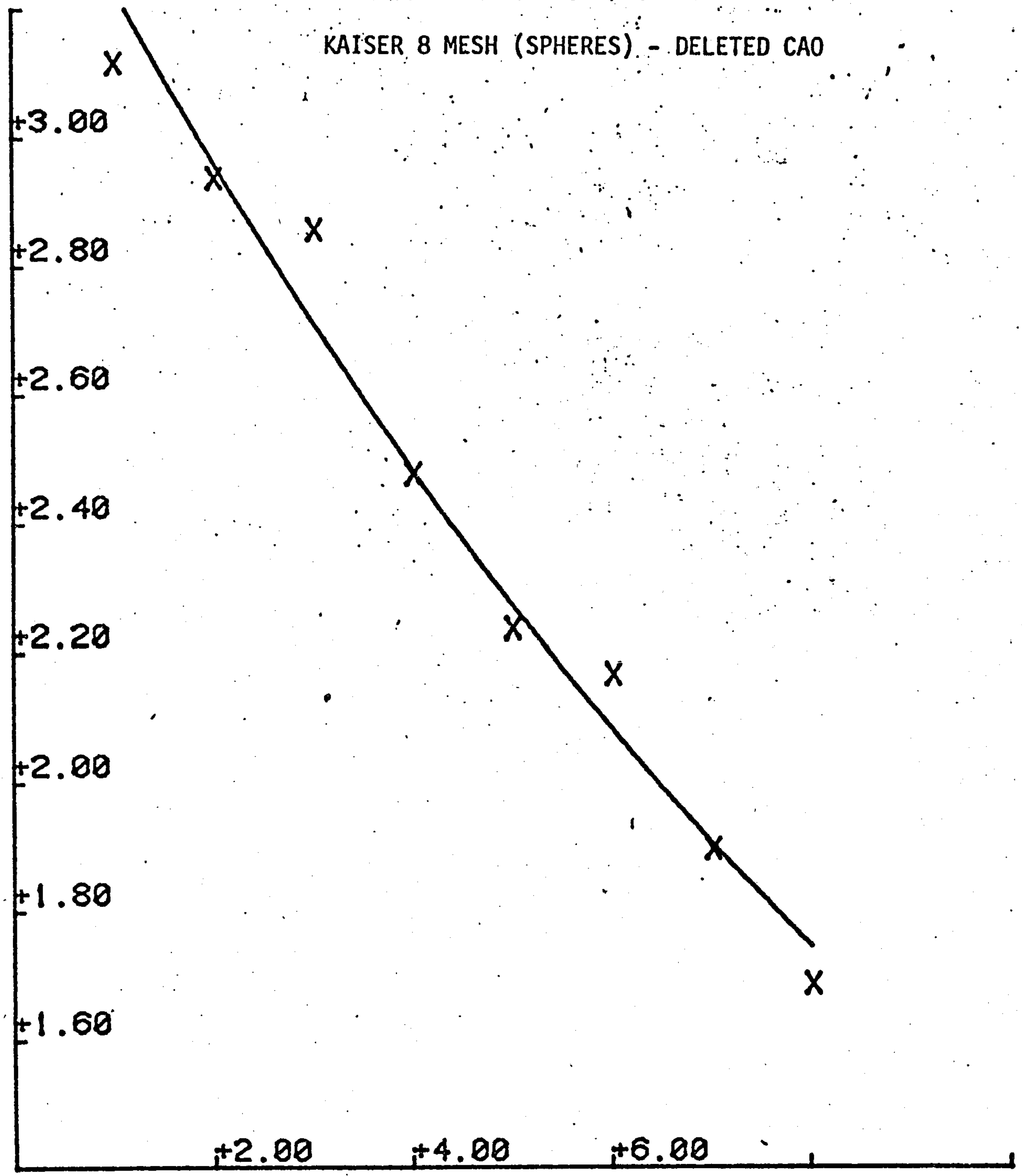

FIGURE 18: SURFACE AREA EFFECT ON KINETIC RATE EXPRESSION CORRELATION COEFFICIENT

MCB (CRUSHED SPHERES) - DELETED CAO

Y = A*EXP(B*X)

A =
3.25475071848

B =
-0.168426343591

R-SQUARE =
0.985702993755

RES ERROR
0.00756506516408

MAX(ABS(RESIDUAL))
0.164780620419

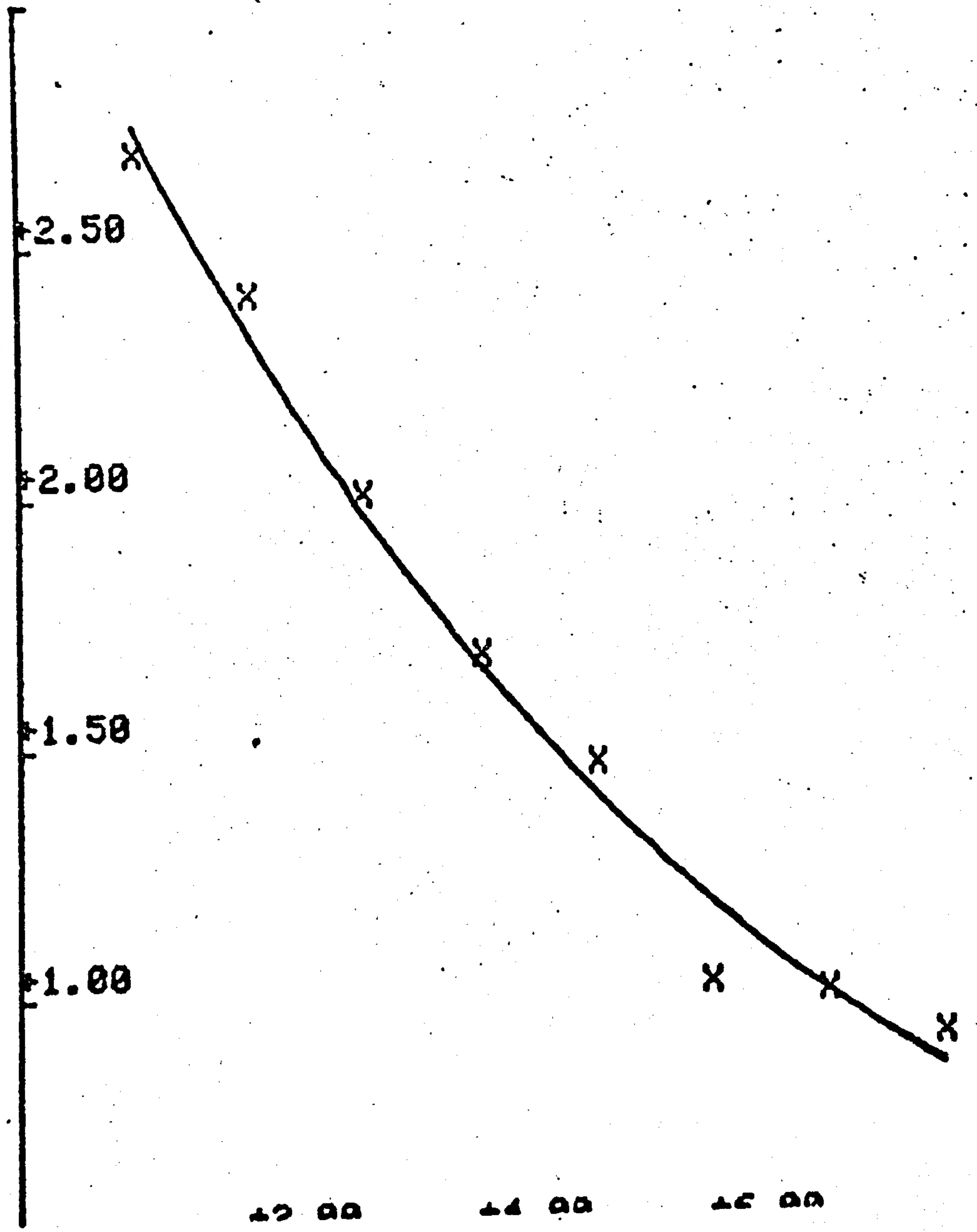

FIGURE 19:

Y = A*X^B

A =
1.59655400681

B =
-0.177275542473

R-SQUARE =
0.979413277738

RES ERROR
6.679962484E-4

MAX(ABS(RESIDUAL))
0.045980879383

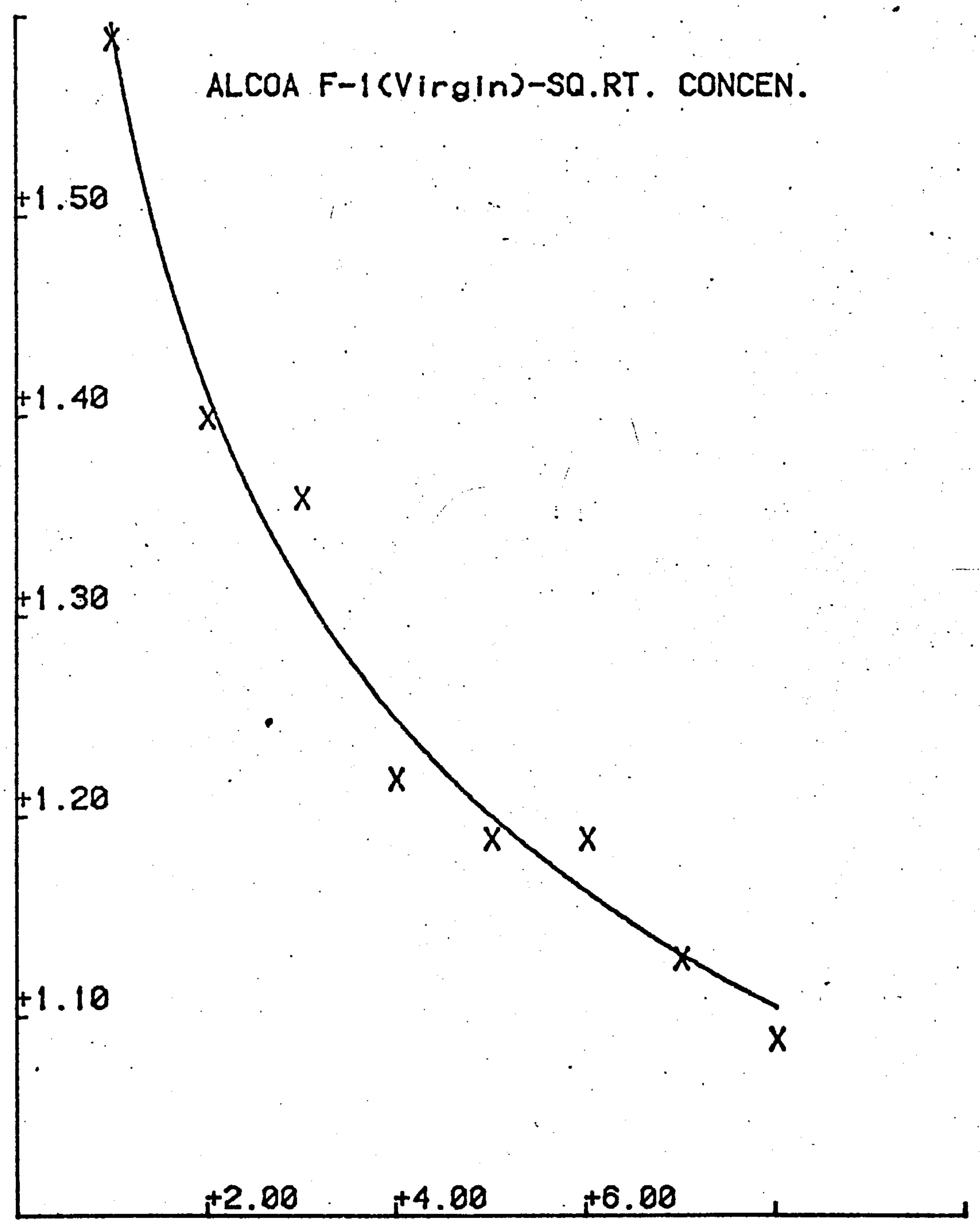

FIGURE 20:

Y = A*X^B

A =
1.76160785782

B =
-0.0428547039272

R-SQUARE =
0.98757451959

RES ERROR
3.769062391E-5

MAX(ABS(RESIDUAL))
0.0106633557477

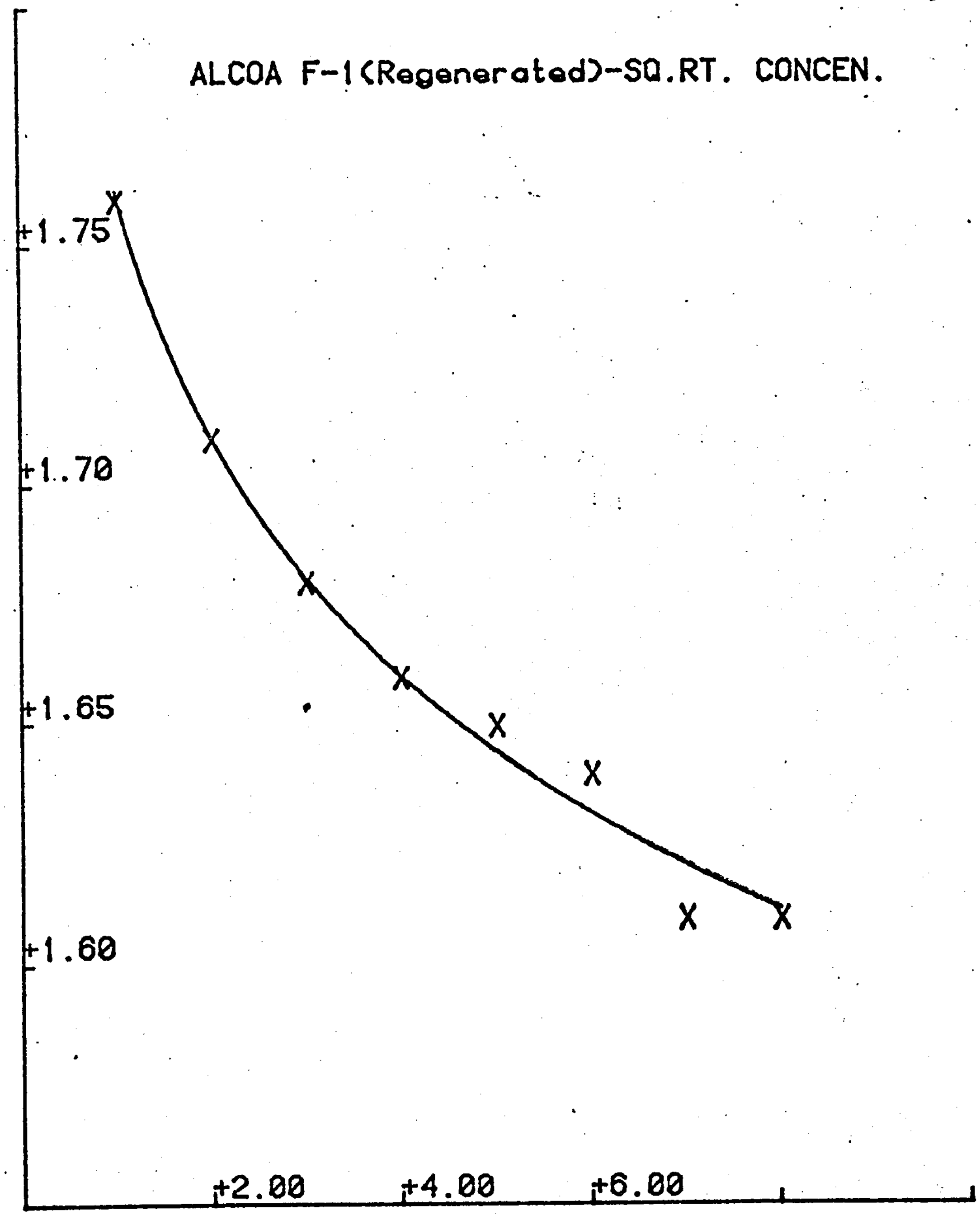

FIGURE 21:

Y = A*X^B

A =
1.17623909209

B =
-0.207245174192

R-SQUARE =
0.944371373405

RES ERROR
0.00138003496857

MAX(ABS(RESIDUAL))
0.0537302203461

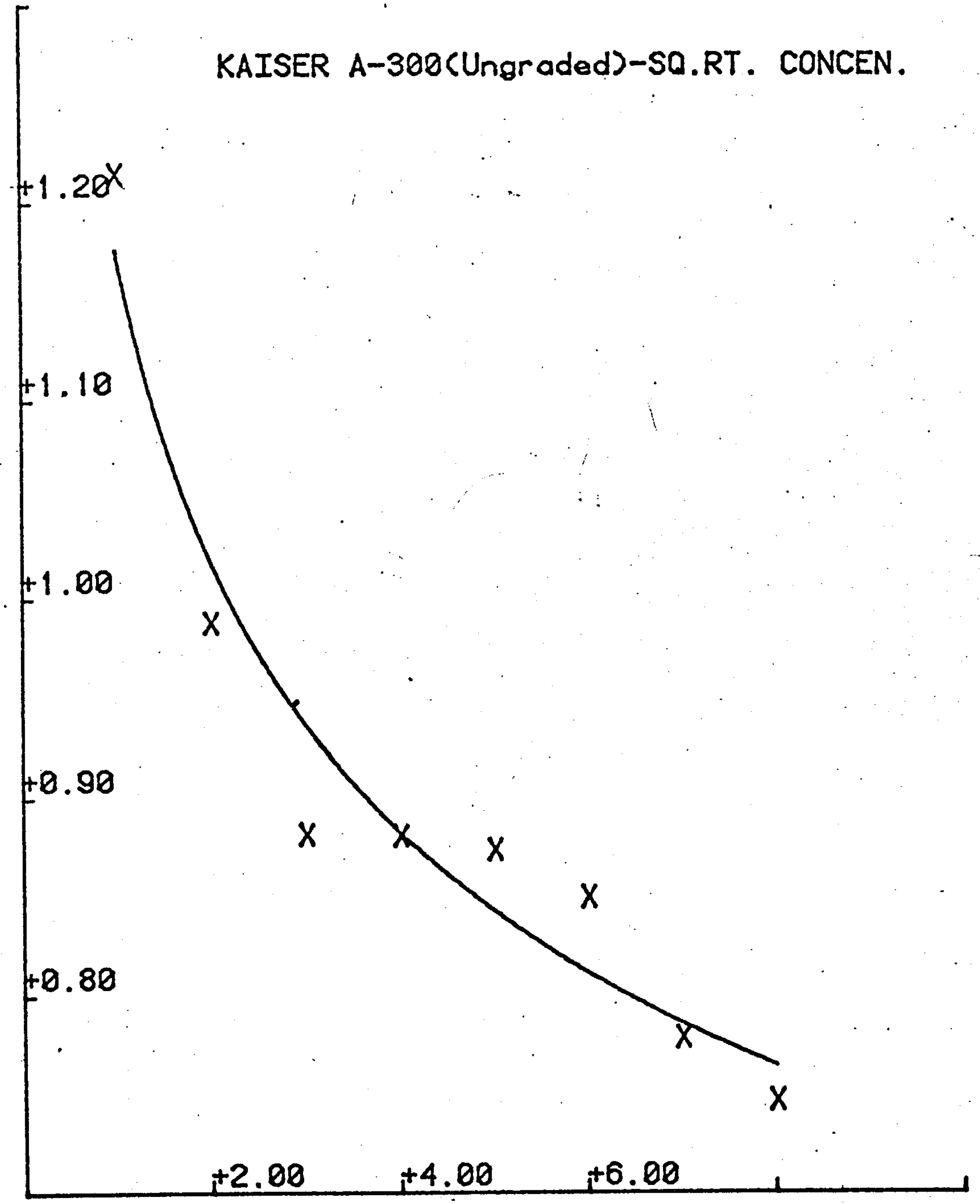

FIGURE 24;

A =
0.758141426723

B =
-0.0726143816953

R-SQUARE =
0.909555764927

RES ERROR
2.02368976E-4

MAX(ABS(RESIDUAL))
0.0161359584475

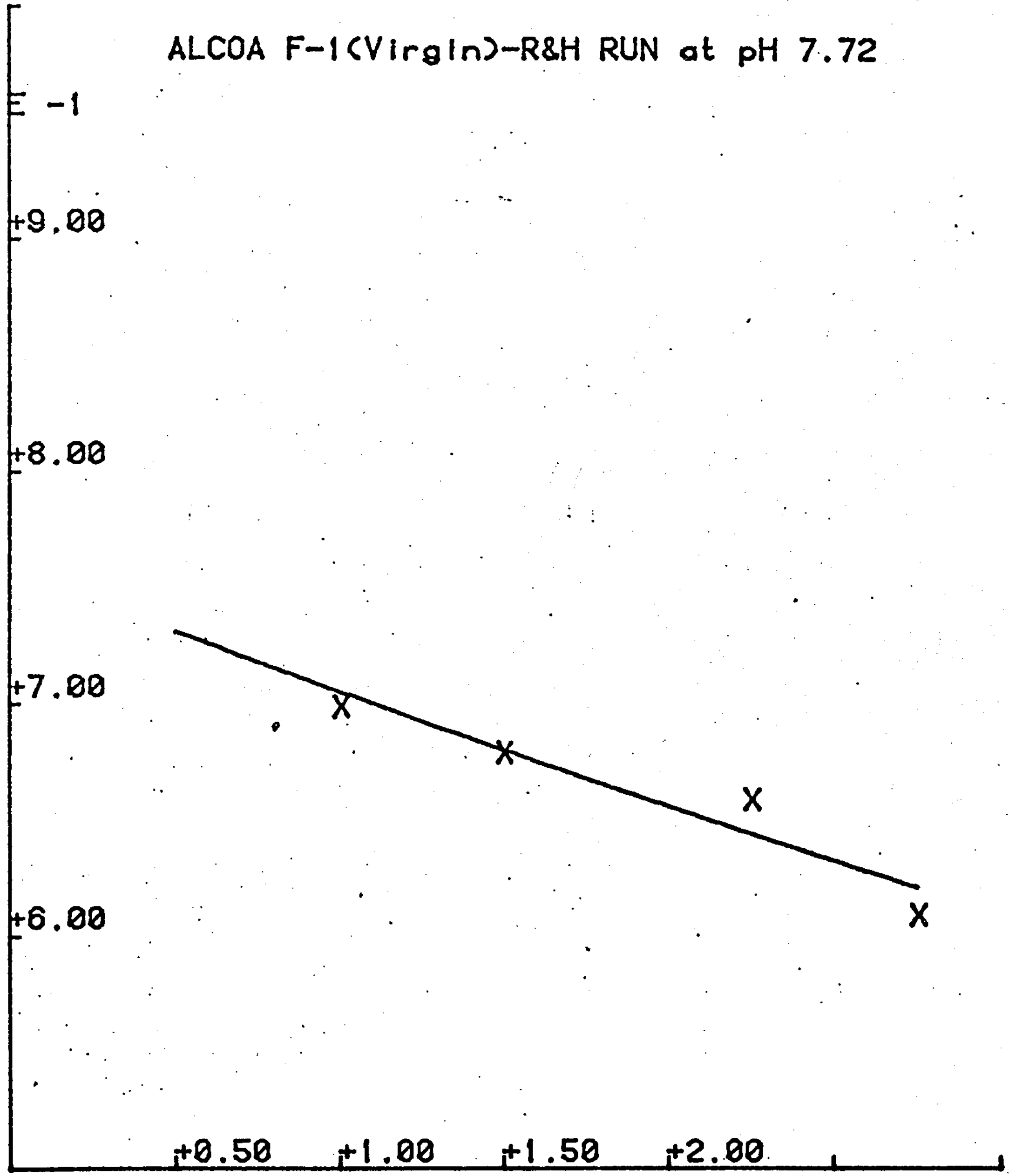

FIGURE 25:

Y = A + B*X

A =
1.434

B =
-2.02285714286

R-SQUARE =
0.984640129417

RES ERROR
0.0174541428571

MAXCABSCRESIDUAL))
0.140285714286